Int J. Multiphase Flow Vol 11, No. 5, pp. 629–641, 1985
Printed in Great Britain

0301-9322/85 $3.00 + .00
Pergamon/Elsevier

PREDICTION OF BUBBLE CONCENTRATION PROFILES IN VERTICAL TURBULENT TWO-PHASE FLOW

STEVEN W. BEYERLEIN,† RAINER K. COSSMANN‡ and HORST. J. RICHTER
Thayer School of Engineering, Dartmouth College, Hanover, NH 03755, U.S.A.

(*Received* 29 *July* 1984; *in revised form* 22 *February* 1985)

Abstract—In vertical bubbly flow, the bubbles are not distributed evenly across the flow section. Several investigators have observed a wall-skewed bubble concentration profile in a vertical upward flow. This paper presents an analysis that predicts this type of bubble distribution by incorporating into the equation of motion a lateral force due to the relative velocity of the two phases and the eddy diffusivity of the liquid. Comparison of analysis and experiment shows good agreement.

1. INTRODUCTION

Bubbly flow is one of the flow regimes in which lateral mixing is significant and the assumption of uniform void distribution is untenable. In particular, transverse phase separation and mixing are likely to be important during boiling, as well as in many chemical engineering processes.

Some investigators have proposed a power law distribution of the discontinuous bubbly phase with a maximum occurring at the flow centerline. Yet quite a number of experiments have shown that in some cases the highest void concentration in upward cocurrent flow exists close to the boundary of the flow section. This has been observed under laminar as well as turbulent conditions.

In this paper, a lateral bubble transport model is developed, which can be used to derive the concentration profile downstream of particular inlet and boundary conditions. This model is tested against experimental results obtained in a 5.1-cm-diameter vertical pipe. The experiments support the theory at very low void fractions. As the bubble concentration increases, lateral migration of bubbles toward the wall of the flow channel is less pronounced owing to the interference imposed by the wake of the one bubble on the flow field around the succeeding bubble.

2. PREVIOUS WORK

Bankoff (1960) assumed that particles and also voids distribute in a fluid flow according to a power law distribution similar to a fluid velocity profile. Zuber (1960) confirmed this distribution. Their data support the notion of a centerline maximum, but the experiments were conducted at average gas void fractions of >20%. This high value corresponds usually to the bubble-slug flow regime where interactions between bubbles and agglomerations thereof are highly significant.

In contrast, Lackmé (1967) observed in his experiments at low void fractions (<10%) bubble motion from the flow centerline to the walls in vertically upward bubbly flow in a 3.2-cm-diameter pipe. This lateral migration was completed within 30 pipe diameters downstream of the bubble injection, becoming more pronounced as the liquid flow rate was increased from a fluid Reynolds number of 6000–22,000. Baker & Chao (1963) reported bubbles rebounding off the channel walls toward the center of the flow section at very high fluid Reynolds numbers ($>10^5$). These investigators also noted that the bubbles remaining on the walls traveled much slower than those in the core. They theorized that this effect stems from the influence of the liquid velocity profile on the bubble trajectory.

†Present address: Stone & Webster Engineering, Boston, Massachusetts, U.S.A.
‡Present address: Rheinisch-Westfälische Technische Hochschule Aachen, Germany.

Kobayasi *et al.* (1970) proposed from their experiments an empirical correlation from which fully developed void fraction profiles can be obtained. For average bubble void fractions of <10%, experiments showed a saddle-shaped wall-skewed bubble distribution. Their empirical correlation offers no insight into the physical phenomena involved in lateral bubble transport.

Similar void distributions were verified by Subbotin *et al.* (1971) in their experiments. Wallis & Richter (1973) postulated first that the relative density of the phases in conjunction with the fluid velocity gradient decided the direction of the transverse motion. Experiments in a 0.025-m square water channel showed that bubbles aggregated at the channel wall in upward cocurrent flow and in the channel center in downward cocurrent flow. The qualitative explanation proposed by these authors for the lateral migration is that the liquid passing by either side of the bubble does so with unequal velocities owing to the fluid velocity gradient. This nonuniformity produces a circulation around the bubble, which gives rise to a lateral force (see figure 1). Extending this explanation to negatively buoyant situations, then, the observations of Young (1960) are consistent with the Wallis & Richter findings (1973).

Rouhani (1976) surmised that periodic dissipation of energy in the laminar sublayer generates rolling vortices. He hypothesized that in two-phase flow, bubbles are centers of rotation and experience radial acceleration. These assumed accelerations are many times the gravitational constant, and should exist also in downward flow; thus, one should witness the same effect on bubble motion independent of the flow direction. This theory contradicts the observations of Wallis & Richter (1973).

3 TRANSPORT MODEL

Zun *et al.* (1975) modified the classical solution for a rotating sphere cited by Schlichting (1979):

$$\vec{f}_m = C\rho_L \vec{V}_{rel} \times \vec{\omega}, \qquad [1]$$

where $\vec{f}_m$ is a lateral force per unit volume, $\vec{\omega}$ is some angular velocity of the bubble, $\vec{V}_{rel}$ is the relative velocity of the bubble, ρ_L is the fluid density and C is a constant of the order unity. If the void fraction is small, the relative velocity V_{rel} is equal to the rise velocity V_∞ of a small bubble in a large quiescent container. The relative velocity on one side of the bubble is then $(V_\infty - \bar{d}_b/2 \cdot \partial V_L/\partial r)$ and on the other $(V_\infty + \bar{d}_b/2 \cdot \partial V_L/\partial r)$ where $\partial V_L/\partial r$ is the fluid velocity gradient in the flow channel at a distance r from the center and $\bar{d}_b$ is the bubble diameter (see figure 2). It can be questioned if [1] is valid at all for bubbles. Clift *et al.* (1978) showed that the motion of bubbles is closely approximated by the motion of spheres in

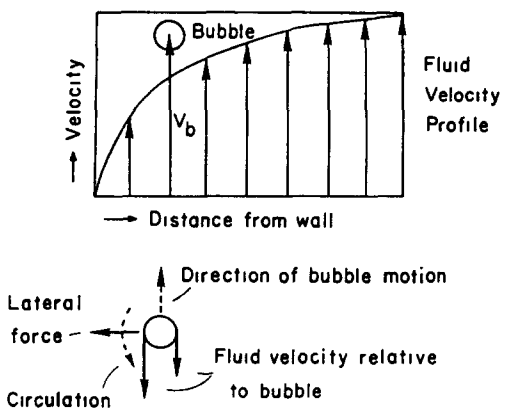

Figure 1. Fluid velocity profile and flow around bubble.

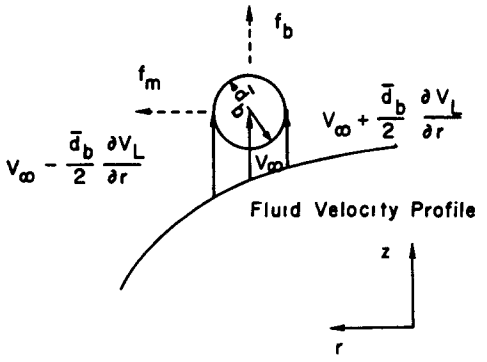

Figure 2. A bubble moving relative to a shear flow.

the presence of even small quantities of surface-active contaminants. In addition, only under the assumption of validity of this equation can we predict the measured void fraction profile.

The angular velocity of the bubble can be approximated as

$$\omega \sim -\frac{\partial V_L}{\partial r}. \qquad [2]$$

Actually, the value of ω will probably be less than this by a factor C_W, since not all points on the surface of the bubble are favorably oriented to produce rotation and the interface velocity of a bubble is not necessarily zero owing to internal circulation.

Laville (1979) measured the motion of striped buoyant styrofoam spheres in a vertical water channel by cinephotography and found qualitatively the trend of [2]. Figure 3 displays Laville's data (1979) and [2] combined with [15], which will be discussed later.

Peck (1973), Zun *et al.* (1975) and Serizawa *et al.* (1975) as well as Sato & Sekoguchi (1975) expressed the opinion that turbulence in the liquid phase superimposes a dispersion

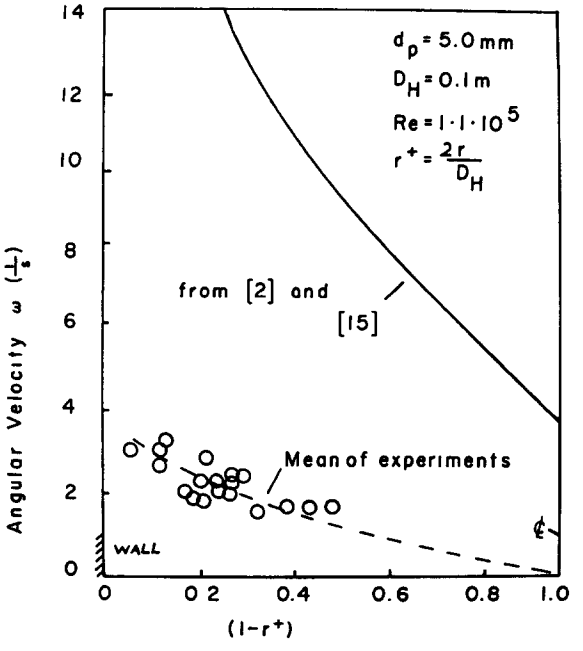

Figure 3. Particle rotation as a function of distance from the wall. Comparison of experimental results with buoyant spheres and [2] and [15].

on the bubble motion. Zun *et al.* (1975) conceived bubble transport in terms of this lateral force plus a bubble dispersion (diffusion) coefficient D_b.

Assuming a certain bubble injection point, Zun *et al.* were able to calculate the developing downstream bubble concentration profile numerically. The transverse bubble velocity can be evaluated easily. Zun *et al.* considered the net force per unit volume. This consists of a lateral force in the transverse direction plus the buoyancy force in the axial direction. This lateral force per unit volume is

$$\vec{f}_m = C\rho_L \vec{V}_\infty \times \vec{\omega}, \qquad [3]$$

or with [2]

$$f_m = - C_t \rho_L V_\infty \frac{\partial V_L}{\partial r}, \qquad [4]$$

where $C_t = C \cdot C_w$. The buoyancy force in a vertical channel per unit volume is

$$f_b = (\rho_L - \rho_G)\, g\,. \qquad [5]$$

Thus, the line of action of the resultant force is oriented at an angle θ to the vertical, where

$$\tan\theta = \frac{-C_t V_\infty (\partial V_L/\partial r)}{g} \qquad [6]$$

if we assume that $\rho_L \gg \rho_G$.

Tan θ is also the ratio of the bubble radial velocity V_r to the bubble rise velocity; thus

$$V_r = \frac{-C_t V_\infty^2 (\partial V_L/\partial r)}{g}. \qquad [7]$$

Therefore, the volumetric bubble flux $\vec{j}$ in cylindrical coordinates is

$$\vec{j} = j_b \vec{r} + j_b \vec{z} = \left(\alpha V_r - \epsilon_b \frac{\partial \alpha}{\partial r}\right)\vec{r} + [\alpha(V_L + V_\infty)]\,\vec{z}, \qquad [8]$$

where $\vec{r}$, $\vec{z}$ are the unit vectors in the radial and axial directions, α is the gas void fraction, V_t is the radial bubble velocity and ϵ_b is the eddy bubble diffusivity.

If bubbles are conserved and thus no breakup or bubble coalescence occurs, then $\nabla\vec{j} = 0$.

Equation [8] can be solved for the axial change in the void fraction profile:

$$\frac{\partial \alpha}{\partial z} = - \frac{1}{r(V_L + V_\infty)} \cdot \frac{\partial}{\partial r}\left[r\left(\alpha V_r - \epsilon_b \frac{\partial \alpha}{\partial r}\right)\right]. \qquad [9]$$

Equations [7] and [8] allow one to calculate the change of concentration profile downstream from an initial profile, provided that the fluid velocity profile can be assumed to be undisturbed by the presence of the bubbles. This restricts the considerations to small void fractions, as will be discussed later. Furthermore, it is necessary that suitable expressions can be determined for the eddy bubble diffusivity ϵ_b as well as the parameter C_t.

C_t is a function of the bubble concentration, since the wake of a preceding bubble will influence the circulation around the succeeding bubble if the bubble concentration is high enough.

Turbulence is expected to have a major influence on lateral bubble diffusion. Therefore, one would anticipate an eddy diffusivity ϵ_b in the transport equation rather than a dispersion coefficient.

Drew & Lahey (1981) used the phasic continuity and momentum equations to show that the void profile can be derived, if one knows the turbulent kinetic energy of the liquid. However, to evaluate the precise radial profile, the anisotropy of the flow must be known.

Serizawa *et al.* (1975) undertook an experimental study of turbulent air–water flow upward in a vertical pipe. They measured bubble distribution, bubble velocity, the fluid velocity as well as turbulent fluctuating velocities. They discovered that the void fraction profile changed from a wall-skewed one to one with a maximum in the center when the overall bubble concentration was increased.

Sato & Sekoguchi (1975) related the shear stress in the liquid to the phase and velocity distribution and suggested a momentum diffusivity for the liquid ϵ_{mL}:

$$\epsilon_{mL} = K_L \frac{R}{6}\left(\frac{\tau_w}{\rho_L}\right)^{1/2}\left[1 - \left(\frac{r}{R}\right)^2\right]\left[1 + 2\left(\frac{r}{R}\right)^2\right], \qquad [10]$$

where K_L is the mixing length constant, commonly taken as $K_L \simeq 0.4$, τ_w is the wall shear stress and R is the pipe radius.

If the single phase-friction factor is introduced, we get for the shear stress

$$\left(\frac{\tau_w}{\rho_L}\right)^{1/2} = \frac{(0.0791)^{1/2}}{Re^{1/8}}\left(\frac{j_L^2}{2(1-\alpha)^2}\right)^{1/2}, \qquad [11]$$

where j_L is the mean liquid velocity, if no bubbles are present, or the so-called superficial velocity of the liquid, and $\bar{\alpha}$ is the average bubble void fraction.

Sato & Sekoguchi (1975) introduced a momentum diffusivity for the gas phase, which is valid only outside of a "bubble sublayer" close to the wall:

$$\epsilon_{mG} = K_G \bar{\alpha} \frac{\bar{d}_b}{2} V_\infty . \qquad [12]$$

In [12] $\bar{d}_b$ is the mean bubble diameter and K_G is an empirical constant, which they assumed to be equal to unity.

According to Sato & Sekoguchi, the two momentum diffusivities can be combined to obtain a two-phase flow eddy diffusivity ϵ_{mTP} in which the shear stresses inside the bubble are neglected:

$$\epsilon_{mTP} = (1 - \bar{\alpha})(\epsilon_{mL} + \bar{\alpha}\epsilon_{mG}) . \qquad [13]$$

The factor $(1 - \bar{\alpha})$ indicates the probability that the liquid phase exists at the point of consideration. In the bubbly flow, where the void fraction is small, the liquid momentum diffusivity dominates the gas diffusivity, and thus ϵ_{mTP} is seen to increase almost linearly with the liquid velocity, with a maximum halfway between the centerline and the wall of the pipe.

The model proposed by Zun *et al.* (1975) can be modified to include the eddy diffusivity introduced by Sato & Sekoguchi (1975), thus linking the bubble dispersion directly to the two-phase momentum diffusivity. This is accomplished by introducing an eddy diffusivity for the bubble transport,

$$\epsilon_b = K_b \epsilon_{mTP}, \qquad [14]$$

where K_b is a constant of the order unity, the particular value of which is explained later. This bubble diffusivity together with the lateral force determines not only the equilibrium bubble concentration but also the rate at which bubbles are transported laterally in the flow conduit. It cannot be surmised at this point that K_b is a true constant. It could be argued that it is a function of the void fraction and/or the developing flow. In the comparison of our low void fraction experiments with the analysis, we found a representative constant satisfactory.

At low bubble concentration, it can be assumed that the liquid velocity profile $V_L(r)$ is essentially identical to single-phase flow.

According to Schlichting (1979), the following relationship is used for the liquid velocity profile,

$$V_L = \frac{j_L}{(1-\bar{\alpha})} \frac{(n+1)(2n+2)}{2n^2} \left(1 - \frac{r}{R}\right)^{1/n}, \qquad [15]$$

where j_L is the volumetric liquid flux, $\bar{\alpha}$ is the average void fraction, R is the pipe radius, and n is a coefficient depending upon the Reynolds number. In addition, the bubble rise velocity V_∞, which is a function of the bubble diameter, was defined as developed by Wallis (1974). Given these equations, the profile development downstream of a particular initial bubble profile can be calculated. The disadvantage of [15] is that its derivative $\partial V_L/\partial r$, which is needed in [2] for the evaluation of the angular velocity, is not zero in the center of the flow conduit (see figure 3).

A finite difference computational scheme was developed by Beyerlein (1981) utilizing [7–14] that allowed the bubble profile developments to be calculated in radially symmetric upward cocurrent flow. In this model, the assumption is that bubbles are conserved, thus no bubble coalescence or breakup occurs. The model yields the same results as the momentum diffusivity concept developed by Quarmby & Anand (1969) when the lateral force and the relative velocity terms are suppressed (figure 4). Both models compare favorably with experiments conducted by Quarmby & Anand in which they released nitrous oxide gas in the center of a circular wind tunnel and measured the radial concentration of the gas as it was carried downstream.

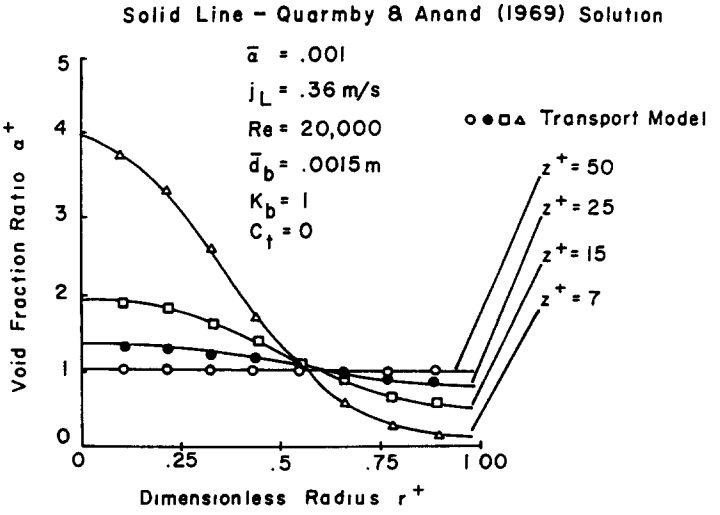

Figure 4. Radial diffusion from a point source. Analytical solution of Quarmby & Anand (1969) for two different gases in comparison with this transport model without the lateral force due to circulation.

The parameters in figure 4 are made nondimensional in the following way:

$$\alpha^+ = \frac{\alpha(r)}{\bar{\alpha}}, \qquad [16]$$

where α is the average void fraction,

$$r^+ = \frac{r}{R} \qquad [17]$$

where R is the pipe radius, and

$$z^+ = \frac{z}{2R} \qquad [18]$$

These dimensionless parameters are used in all succeeding plots of profile developments.

The parameter C_t in the equation for the circulation around the sphere and the constant K_b in the momentum diffusivity term must be determined empirically. If both are set arbitrarily to 0.5, the qualitative profile development behavior of bubbly flow can be assessed. In these studies, it was found that at small average void fractions ($\bar{\alpha} \leq 0.001$), the lateral bubble migration toward the wall is slightly accelerated when the liquid flow rate is increased. However, these effects are nowhere near as appreciable as those witnessed when the bubble size, and implicitly the bubble relative velocity, is altered.

Figures 5 and 6 show the bubble concentration profile for the same average void fraction and liquid velocity, only the bubble diameter is changed from 1 to 2 mm in figure 6. In the latter case, the bubble migration toward the walls is enhanced considerably.

In these sensitivity studies, C_t and K_b were assumed to be independent of flow variables. As mentioned earlier, if bubble–bubble interactions occur and the bubbles disturb the liquid velocity profile and turbulence structure of the flow substantially, this theory ceases to be a useful predictive tool. This probably takes place before the flow regime changes to slug flow.

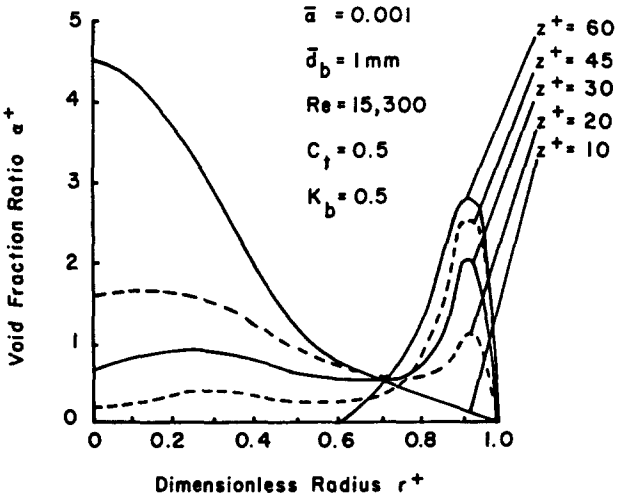

Figure 5. Prediction of bubble void fraction profile developments as a function of distance from the bubble injection point from this transport model.

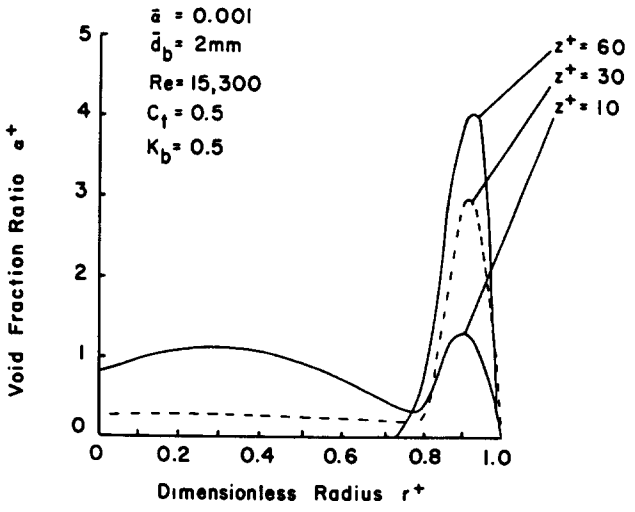

Figure 6. Prediction of bubble void fraction development as a function of distance from the bubble injection point from this transport model. In comparison with figure 5, the bubble diameter is increased from 1 to 2 mm.

4. EXPERIMENTS

In order to verify the present model, an experimental facility was built. This consisted of a vertical 5.1-cm-internal diameter Plexiglas type ~2.5 m long (figure 7). Care was taken to minimize the vorticity entering the test section by passing the fluid through layers of sponge, screen and honeycomb. Air bubbles were injected in the pipe and the ensuing void distributions were recorded at several cross sections downstream of the injection point.

Two single-bubble injectors were constructed, which allowed the release of a continuous stream of individual bubbles of different size at the pipe centerline. A somewhat different bubble generator was constructed to accommodate higher void fractions. Solnit (1981) built a bubble generator to be installed in the entrance of the test section consisting of a container with a top plate with ~40 orifices. This container was connected to an air supply via a fast-oscillating solenoid valve. About 1600 bubbles/s could be released from this device.

The size of the bubbles from all these devices was measured by evaluating the gas flow rate and the bubble frequency. It was necessary to measure the bubble size and frequency at

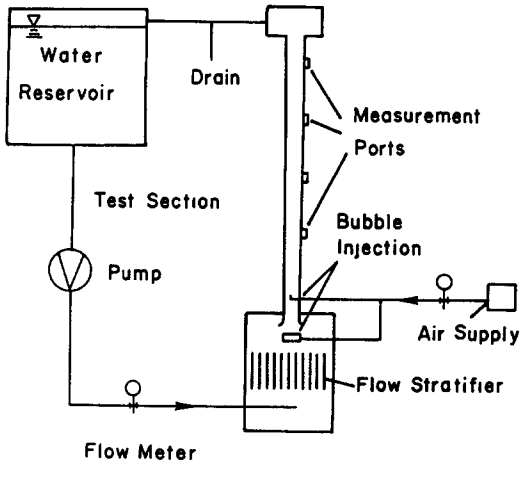

Figure 7. Test facility.

all liquid flow velocities, since at higher velocities the bubbles were pulled away earlier from the top of the generator during bubble growth.

Monitoring the local bubble concentration was found to be not a trivial task. An intrusive conductivity probe formed like a needle was developed, and the change in the conductivity due to the presence of a bubble could be detected. The sensing diameter of this probe was calibrated very carefully as described by Beyerlein (1981). In each location, usually a time averaging was necessary, at very low void fractions. This time averaging could be in the range of 1 min or so.

5. EXPERIMENTAL RESULTS AND COMPARISON WITH THE PRESENT MODEL

In the experiments, the bubble void fraction was measured axially and radially at several locations downstream from the bubble injection. The measurements were performed for different liquid volumetric fluxes and different average bubble void fractions.

Comparison of the experimental results with the theory developed in section 3 indicated that the parameter in the mixing length in [14] can be treated as a true constant, at least in the range of experiments performed here, its value being $K_b = 0.3$, but the parameter C_t in the lateral force [7] was found to be a function of the average void fraction and the liquid Reynolds number. As mentioned earlier, it can be expected that with an increase in void fraction, the importance of the lateral force will decrease owing to interaction between bubbles. Thus, the parameter C_t should decrease with an increase in void fraction.

Figures 8–12 show several comparisons of the measured and the predicted void fraction profile in the vertical test section. It should be noted that the measured void profile at $z^+ = 0$ was used as input into the analytical model. The parameter C_t was varied to optimize the agreement of analysis and experiment. Even though a Reynolds number dependency of the parameter was expected, it could not be deduced clearly, since in these experiments the Reynolds number was changed only from $\sim 10^4$ to 6×10^4, owing to limitations in the test facility. Therefore, C_t was evaluated only as a function of the average void fraction. From all test results, the parameter in the lateral force equation was plotted in figure 13 and defined empirically as

$$C_t = 1.65 \times 10^{-3} \alpha^{-0.78}. \qquad [19]$$

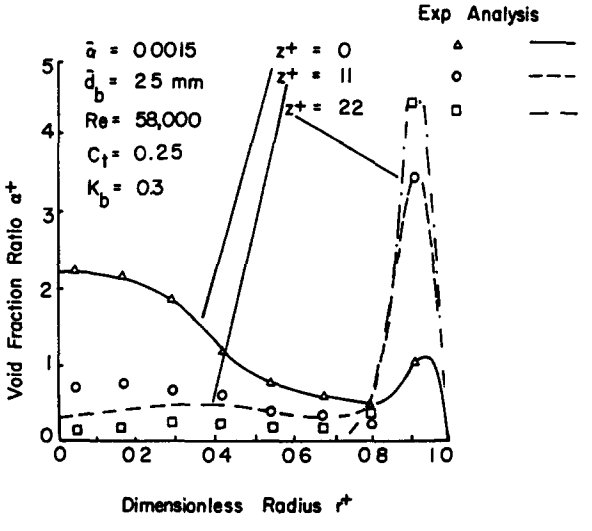

Figure 8. Comparison of measurements and analytical predictions of the void fraction ratio α^+ versus dimensionless radial position r^+ in the pipe as a function of the dimensionless downstream position z^+.

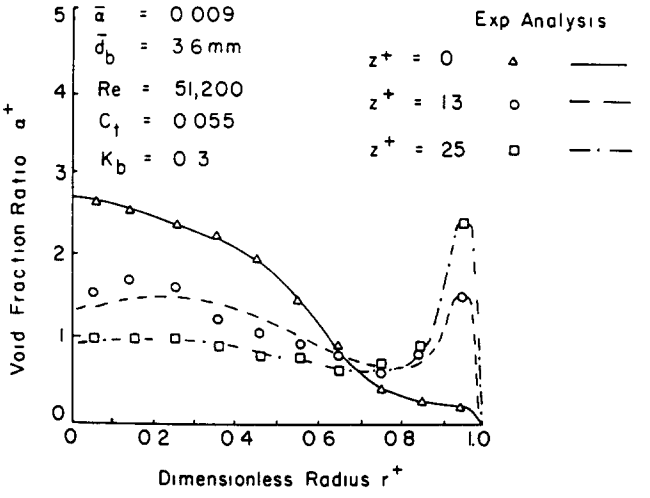

Figure 9. Comparison of measurements and analytical predictions of the void fraction ratio α^+ versus dimensionless radial position r^+ in the pipe as a function of the dimensionless downstream position z^+.

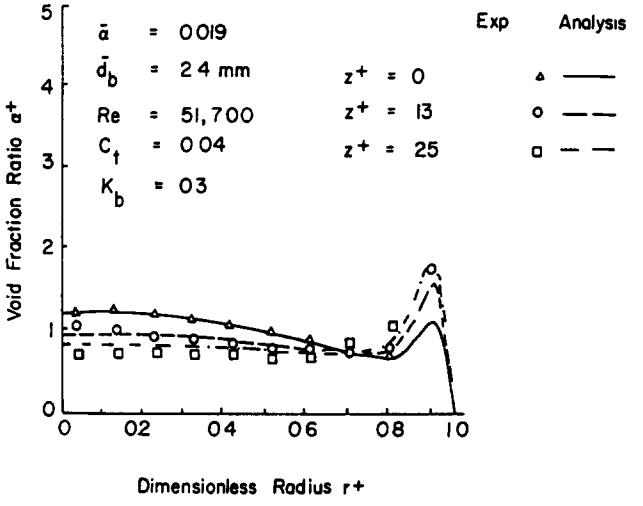

Figure 10. Comparison of measurements and analytical predictions of the void fraction ratio α^+ versus dimensionless radial position r^+ in the pipe as a function of the dimensionless downstream position z^+.

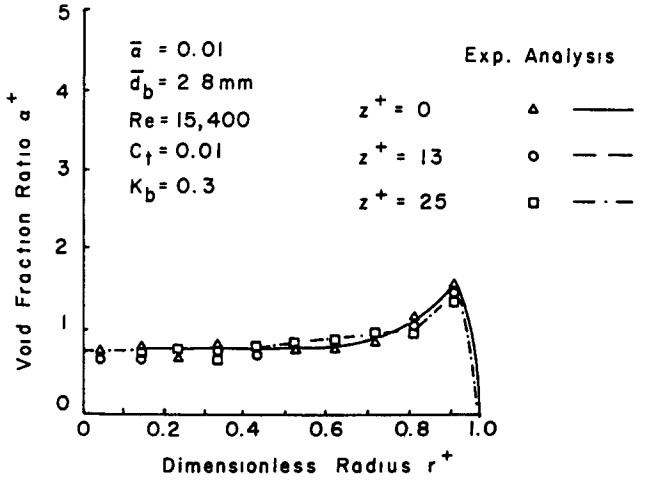

Figure 11. Comparison of measurements and analytical predictions of the void fraction ratio α^+ versus dimensionless radial position r^+ in the pipe as a function of the dimensionless downstream position z^+.

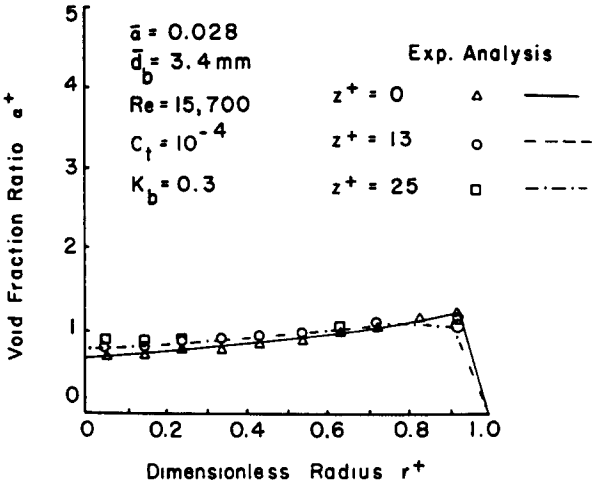

Figure 12. Comparison of measurements and analytical predictions of the void fraction ratio α^+ versus dimensionless radial position r^+ in the pipe as a function of the dimensionless downstream position z^+.

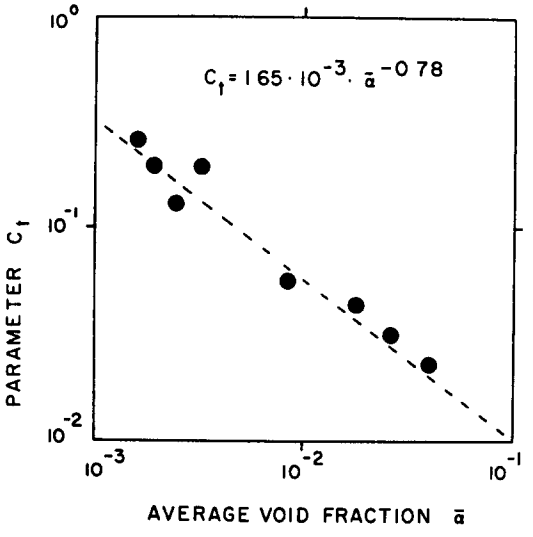

Figure 13. Parameter C_f as a function of the average void fraction.

It is interesting to note that at very low void fractions, the parameter C_f has a similar value to the one obtained from solid sphere experiments, suggesting that internal circulation is probably not important in bubbles of this size. The wall-skewed void profile disappears at higher void fractions as contemplated (see figure 12).

It is obvious that [19] is not generally valid. Many more data points in different geometries, at different flow rates as well as at different void fractions are necessary in order to draw more general conclusions. But in spite of the limited data, [19] shows the expected trend.

6. CONCLUSIONS

Multidimensional effects are important in upward cocurrent flow. This can be seen clearly in the experimental results obtained during the course of this work. It was found that at low void fractions, bubbly flow evolves toward a wall-skewed bubble distribution. This process is enhanced with an increase in fluid velocity and/or bubble diameter.

Radial bubble migration in turbulent flow is claimed to be a product of a circulation-induced lateral force and bubble diffusion. The former is due to interplay of buoyancy and the fluid velocity gradient, the latter is actuated by the turbulence in the flow.

The coupling of the lateral force with bubble diffusion derived from the mixing length theory results in a model capable of predicting the developing void profile.

Further refinement of this model requires consideration of the flow structure surrounding individual bubbles. In addition, a better definition of the relative bubble velocity is needed close to the wall of the conduit. This was considered in this model by introducing a parameter into the lateral force equation, which is assumed to be a function of the average void fraction and the liquid Reynolds number. In view of the parameter introduced, the agreement of the analytical predictions and experimental results is good in the described low voidage range, as one would expect. The dependency of the parameter on the average void fraction could be clearly deduced.

This work is considered to be a first step in the direction of understanding the wall-skewed bubble void profile in vertical two-phase flow. More detailed studies in the vicinity of individual bubbles and at higher void fractions are needed before a better analytically based correlation can be found.

Acknowledgements—This work was supported by the National Science Foundation (NSF) under the Fluids Division Program, Project Director Dr K. Lea. Aaron Solnit developed a bubble generator that allowed experiments at higher void fractions and made extensive experiments.

REFERENCES

BAKER, J. L. L. & CHAO, B. T. 1963 An experimental investigation of bubble motion in turbulent liquid stream. University of Illinois ME Technical Report, 1069–1.

BANKOFF, S. G. 1960 A variable density single-fluid model for two-phase flow with particular reference to steam-water flow. *Trans. ASME J. Heat Transfer* **82,** 265–272.

BEYERLEIN, S. W. 1981 Mechanisms of bubble transport in turbulent flow. M.S. thesis, Thayer School of Engineering, Dartmouth College, Hanover, NH.

DREW, D. A. & LAHEY, R. T. 1981 Phase distribution mechanisms in turbulent two-phase flow in channels of arbitrary cross section. *J. Fluids Engng* **103,** 583–589.

KOBAYASI, K., IIDA, Y. & KANEGAE, N. 1970 Distribution of local void fraction of air-water two-phase flow in a vertical channel. *Bull. JSME* **13,** 1005–1012.

LACKMÉ, C. 1967 Structure et cinematique des ecoulements diphasiques a bulles. Centre d'Etudes Nucleaires de Grenoble, Report No. CEA, p. 320.

LAVILLE, A. 1979 Lateral particle migration in vertical channel flow. Dartmouth College, Thayer School of Engineering, Hanover, NH.

PECK, V. C. 1973 Influence of walls on bubble motion in nearly vertical flow. Eng. 141 project, Dartmouth College, Thayer School of Engineering, Hanover, NH.

QUARMBY, A. & ANAND, R. J. 1969 Axisymmetric turbulent mass transfer in a circular tube. *J. Fluid Mech.* **38,** 457–492.

ROUHANI, Z. 1976 Effect of wall friction and vortex generation on radial void distribution, the wall-vortex effect. *Int. J. Multiphase Flow* **3,** 35–50.

SATO, Y. & SEKOGUCHI, K. 1975 Liquid velocity distribution in two-phase bubble flow. *Int. J. Multiphase Flow* **2,** 79–95.

SCHLICHTING, H. 1979 *Boundary Layer Theory*. McGraw-Hill, New York.

SERIZAWA, R., KATASHA, I. & MICHIYUKI, I. 1975 Turbulence structure of air-water bubbly flow. I. Measuring technique, II. Local properties, III. Transport properties. *Int. J. Multiphase Flow* **2,** 221–259.

SOLNIT, A. 1981 Personal communication, Dartmouth College, Thayer School of Engineering, Hanover, NH.

SUBBOTIN, V. I., IBRAGINOV, M. K., BOBKOV, V. P. & TYCHINSKI, N. A. 1971 Turbulent channel-flow characteristics of gas-water mixtures. *Soviet Physics-Doklady* **16,** 192–194.

WALLIS, G. B. 1974 The terminal speed of single drops or bubbles in an infinite medium. *Int. J. Multiphase Flow* **1,** 491–511.

WALLIS, G. B. & RICHTER, H. J. 1973 Influence of walls on bubble motion in vertical two-phase flow. Dartmouth College, Thayer School of Engineering, Hanover, NH.

YOUNG, D. F. N. D. 1960 The coring phenomenon in the flow of suspensions in vertical tubes. ASME Paper No. 60-HYD-12.

ZUBER, N. 1960 On the variable density single-fluid model for two-phase flow. *Trans. ASME J. Heat Transfer* **82,** 255–258.

ZUN, I., RICHTER, H. J. & WALLIS, G. B. 1975 The transverse migration of bubbles in vertical two-phase flow. Dartmouth College, Thayer School of Engineering, Hanover, NH.